4th URSI AT-RASC, Gran Canaria, 19 – 24 May 2024

From Propagation Channel to Radio Channel: Beamforming Impact on Millimeter-Wave and Sub-Terahertz Wireless Transmission

Peize Zhang*(1), Katsuyuki Haneda(2), Wei Fan(3), Aarno Pärssinen(1), and Pekka Kyösti(1)(4)
(1) Centre for Wireless Communications, University of Oulu, 90570 Oulu, Finland
(2) Department of Electronics and Nanoengineering, Aalto University, 02150 Espoo, Finland
(3) National Mobile Communications Research Laboratory, Southeast University, Nanjing 210096, China
(4) Keysight Technologies Finland Oy, 90590 Oulu, Finland

Abstract

To design a millimeter-wave/sub-terahertz wireless system, it is essential to understand the radio channel in which it will operate rather than the propagation channel. Radio channel consists of antennas and radio front-ends, in addition to propagation channel. In this paper, a framework of involving beamforming impact for radio channel characterization is introduced using multi-band measured and simulated propagation channel data. On the beamformed channel, we propose a beam direction-based channel similarity metric for the evaluation of multi-band channel similarity, as well as uplink and downlink channel reciprocity. The beamforming impact on time dispersion of measured sub-THz channels is also analyzed for radio interface design and parametrization.

1 Introduction

Future 6G wireless networks will be able to operate in multiple frequency bands, including existing frequency range 1 (FR1) from 410 MHz to 7125 MHz and millimeter-wave (mmWave) FR2 from 24.25 GHz to 52.6 GHz allocated for 5G new radio (NR), as well as the additional spectrum in the essential centimetric range, i.e., 7–20 GHz and the complementary sub-terahertz (sub-THz) range, i.e., 92–300 GHz. The tiny wavelengths for mmWave and sub-THz spectrum facilitate large antenna arrays with hundreds and even thousands of elements to be packed in a compact physical size. The large beamforming gains achievable via 5G massive MIMO and 6G extremely large-scale MIMO technologies can in turn extend the coverage of mmWave/sub-THz networks at longer ranges to overcome the high propagation loss. Since highly directive links are susceptible to blockage dynamics, high probability of beam misalignment requires frequent beam updates, leading to high latency and training overhead for link establishment and tracking [1]. To optimize the system design, it is desirable to exploit the unique properties of the mmWave and sub-THz channels.

Propagation channel is independent of the antennas employed at both link ends. Continuous evolution of channel models from 2G to 5G and toward 6G is mainly because of using new frequencies in new scenarios [2,3]. For example, the common understanding from measurement results that multipath channel becomes sparser and more specular when going higher in radio frequency, and the channel model parameters in [3] were updated accordingly. *Radio channel* consists of propagation channel, antennas, and radio front-ends, where the wireless system actually operates in the radio channel observed via antennas. For example. some new channel characteristics can thus be observed due to the use of large-scale antenna arrays, including favorable propagation, spatial non-stationary, and near-field spherical-wave propagation. For real implementation of large antenna arrays with beamforming in mmWave and sub-THz networks, it is essential to have some quantitative knowledge about the radio channels considering the beamforming impact.

In this paper, we summarize our recent works in radio channel characterization by embedding the practical beam patterns of different antenna arrays in propagation channel and draw insights on low-complexity and low-cost design of mmWave/sub-THz tranceiver systems. First, propagation channel data can be collected via field measurement and ray-tracing simulation [4]. We can obtain the angular information of mmWave/sub-THz propagation channels during measurements by implementing different antennas, e.g., rotating horn antenna in azimuth and elevation planes, moving omnidirectional antennas to form virtual antenna arrays, and real antenna arrays. Furthermore, the path gain, propagation delay, and direction of arrival and departure of each multipath component (MPC) can be estimated, e.g., via high-resolution parameter estimation algorithms. The antenna radiation patterns of the transmitting (Tx) and receiving (Rx) antennas have been de-embedded from the raw measurement data. Once the propagation channel data is collected, we can derive the radio channel by performing circular convolution of the power angular spectrum (PAS) and the antenna pattern generated via specific beamformer, which is defined as *beamformed channel*. As an alternative to derive beamformed channel, beam steering is applied during measurements when using physical antenna arrays or as a post-processing step when using virtual antenna arrays. Finally, the beamforming impact on spatial and temporal channel characteristics are analyzed based on

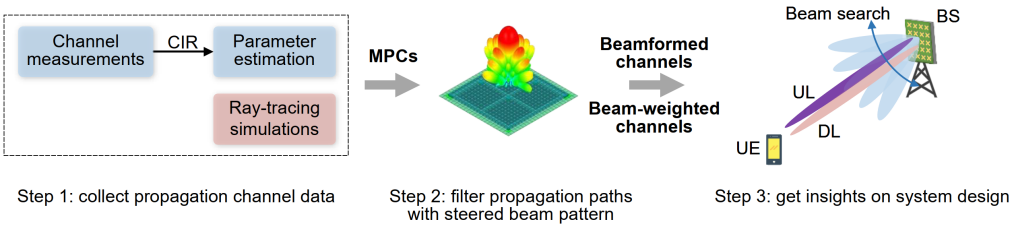

Figure 1. The framework for the analysis of beamforming impact on mmWave and sub-THz wireless transmission using measurement and simulation channel data.

beam-weighted channel, which is introduced by weighting the MPCs of a propagation channel with a steered beam pattern to a specific beam direction. Furthermore, some insights for mmWave/sub-THz wireless transmission scheme design can be drawn from a radio channel point of view.

The rest of the paper is organized as the follows. Section 2 introduces the framework for the analysis of beamforming impact using measurement and simulation channel data. Section 3 describes the details about channel data collection from measurements and ray-tracing simulations. Section 4 discusses the beamforming impact on mmWave and sub-THz wireless transmission from a radio channel perspective. Finally, Section 5 concludes the paper.

2 Framework

A straightforward way to involve beamforming impact in radio channel characterization is to implement different beamforming algorithms on MIMO channel measurement data via post-processing. However, it is challenging to efficiently collect MIMO channel data, especially in sub-THz band, due to the lack of commercial off-the-shelf (COTS) antenna arrays and high implementation costs for channel sounding. Thus, we develop a framework (see Figure 1) for analyzing the beamforming impact on mmWave and sub-THz wireless transmission based on propagation channel data, i.e., MPCs including path gain, propagation delay, and angles of arrival and departure (AoA/AoD).

The first step is to collect propagation channel data from field measurements and ray-tracing simulations. Double-directional multipath propagation channel can be represented via power angular delay profiles (PADPs) as

$$P(\tau,\Omega_{\rm rx},\Omega_{\rm tx})=\sum_{l=1}^{L}p_l\delta(\Omega_{\rm rx}-\Omega_{{\rm rx},l})\delta(\Omega_{\rm tx}-\Omega_{{\rm tx},l})\delta(\tau-\tau_l) \quad (1)$$

where L is the total number of MPCs, $\delta(\cdot)$ is the delta function, p_l, $\Omega_{{\rm rx},l}$, $\Omega_{{\rm tx},l}$, and τ_l are the power, AoA, AoD, and delay of the l-th path, respectively. Note that $\Omega_l=(\theta_l,\phi_l)$ includes both azimuth angle ϕ_l and elevation angle θ_l. Channel parameters $\{L,p_l,\Omega_{{\rm rx},l},\Omega_{{\rm tx},l},\tau_l\}$ can be estimated from measured channel impulse responses (CIRs), or directly extracted from ray-tracing simulations, while the antenna gain has been de-embedded from the raw data.

The second step performs the circular convolution of the steered beam pattern and the power angular spectrum (PAS). For simplicity, we only consider the single-direction PAS with respect to azimuth AoA as:

$$P(\phi_{\rm rx})=\sum_{\tau}\sum_{\Omega_{\rm tx}}\sum_{\theta_{\rm rx}}P(\tau,\Omega_{\rm rx},\Omega_{\rm tx})=\sum_{l=1}^{L}p_l\delta(\phi_{\rm rx}-\phi_{{\rm rx},l}) \quad (2)$$

Then, the PAS of the beamformed channel is calculated as

$$\hat{P}(\varphi_{\rm rx})=\sum_{l=1}^{L}p_l G(\varphi_{\rm rx}-\phi_{{\rm rx},l}) \quad (3)$$

which corresponds to steering the beam pattern $G(\phi_{\rm rx})$ to a direction $\varphi_{\rm rx}$ and collecting the sum power from all observable MPCs weighted with corresponding beam gains. Here, we steer beam towards all azimuth angles $\varphi_{\rm rx}$ in $[0^\circ,360^\circ]$ with the increment of 1°. Figure 2 gives an example of beamformed PAS observed via the beam pattern of half-wavelength-spaced uniform linear array (ULA) with 4 elements.

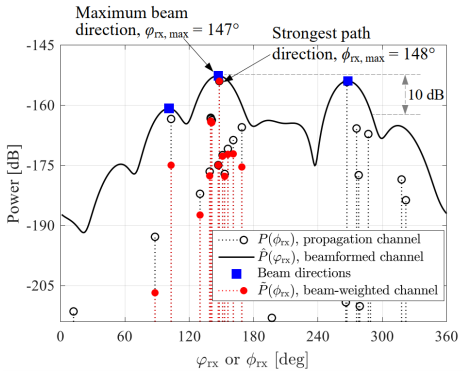

Figure 2. An example of beamformed PAS $\hat{P}(\varphi_{\rm rx})$ calculated based on $P(\phi_{\rm rx})$ of propagation channel.

The final step is to draw design insights based on the beamformed PAS derived from Step 2. For example, three beam directions (blue squares) can be detected from Figure 2, i.e., the local maxima of the beamformed PAS, using peak detection algorithm. Here only the peaks whose powers are within 10 dB threshold relative to the maximum power are taken into account. In [5], we performed statistical analysis of the number of beams that D-band radio channel can support. Besides, we proposed a beam direction-based similarity metric to characterize the similarity level of two radio channels observed by the beam patterns with different half-power beamwidths (HPBWs) [6]. The metric is utilized to

evaluate the feasibility of out-of-band spatial channel information aided mmWave/sub-THz beam search strategy [7], as well as the uplink (UL) and downlink (DL) channel reciprocity when using asymmetric transceiver [8]. Meanwhile, beamforming impact on time dispersion in measured sub-THz radio channels will be analyzed for the purpose of novel waveform and air interface design.

3 Channel Data Collection

3.1 Channel Measurements

Sub-THz channel measurement campaigns across multiple indoor and outdooor scenarios were conducted using vector network analyzer (VNA) based channel sounder at the center frequency of 142 GHz with 4 GHz bandwidth [4]. During the measurement, an omni-directional bicone antenna with 45° elevation HPBW was fixed on the Tx side, while on the Rx side a horn antenna with 10° azimuth HPBW and 40° elevation HPBW was rotated in the azimuth plane with an increment of 5° following the directional scanning sounding method. The Tx and Rx antennas were both mounted at the height of 1.85 m above the ground. The radiation patterns of the bicone and horn antennas were de-embedded from measured directional CIRs in the process of estimating MPCs. Recently, we developed a correlation-based time-domain channel sounder to support sub-THz channel measurements using COTS instruments [9]. Compared with the VNA-based channel sounder, the proposed sounder enables fast and wideband measurements of time-varying channels. Extensive channel measurement activities will be carried out and the measured propagation channel data can be further used for statistical analysis.

3.2 Ray-Tracing Simulations

Since it is challenging to collect measured channel data across multiple frequency bands, e.g., sub-6 GHz, mmWave, and sub-THz, at identical Tx-Rx locations. An alternative is to perform multi-band ray-tracing simulations, where the corresponding outputs include the MPC information in (1). For example, in [7] ray-tracing simulations at five mmWave frequencies (i.e., 4, 15, 28, 60, and 86 GHz) were performed over 2875 Tx-Rx location combinations in Helsinki-Vantaa airport check-in area. The following propagation mechanisms were considered in the simulations, including single- and double-bounce reflections, diffraction, and diffraction-to-reflection. More details about the simulation setup can be found in [7].

4 Analysis and Discussion

4.1 Spatial Channel Similarity

The feasibility of out-of-band spatial channel information aided mmWave/sub-THz beam search strategy depends on the spatial channel similarity across multiple frequency bands [10]. In [7], we developed a beam direction-based spatial channel similarity metric using the estimated beam directions from beamformed PASs of high- and low-frequency (HF/LF) channels, i.e., $\hat{P}_{\mathrm{HF}}(\varphi_{\mathrm{rx}})$ and $\hat{P}_{\mathrm{LF}}(\varphi_{\mathrm{rx}})$, respectively, calculated as:

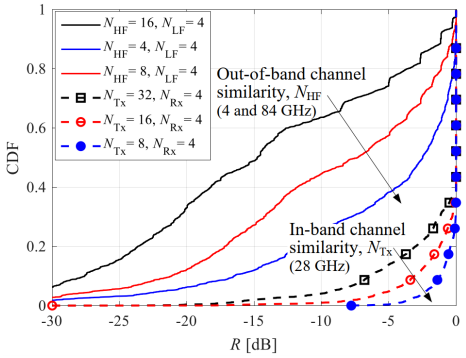

Figure 3. Empirical CDFs of the power ratio metric based on multi-band ray-tracing simulation data.

$$R\,[\mathrm{dB}] = \frac{\sum_{\varphi_{\mathrm{rx}} \in \mathscr{A}_{\mathrm{LF}}} \hat{P}_{\mathrm{HF}}(\varphi_{\mathrm{rx}})}{\sum_{\varphi_{\mathrm{rx}} \in \mathscr{A}_{\mathrm{HF}}} \hat{P}_{\mathrm{HF}}(\varphi_{\mathrm{rx}})}, \tag{4}$$

where $\mathscr{A}_{\mathrm{HF}}$ and $\mathscr{A}_{\mathrm{LF}}$ denote the azimuth angle sets of potential beam directions estimated from HF and LF radio channels, respectively. Shorter wavelength at HF (mmWave/sub-THz) enables to integrate more antenna elements within a compact physical space compared with LF (sub-6 GHz) antenna arrays. Thus, HF directional transmission systems are capable of radiating more sharpened beam patterns than the systems operating at LF. The power ratio R is less than or equal to 0 dB since more beam directions can be detected from the HF radio channel observed by narrower beam pattern in comparison with the LF radio channel observed by wider beam pattern. Empirical cumulative distribution functions (CDFs) of the R values are shown in Figure 3. When using out-of-band spatial channel information at 4 GHz to aid 86 GHz beam search, at worst 2.27 dB, 7.31 dB, and 14.77 dB power losses are introduced in 50% of cases when the ULAs with $N_{\mathrm{HF}} = 4$, 8, and 16 elements are employed at HF, respectively, while we maintain the LF ULA with a constant number of elements, i.e., $N_{\mathrm{LF}} = 4$.

Besides, the proposed similarity metric can be leveraged for analysis of UL and DL radio channel reciprocity when using asymmetric transceiver developed in [8], where the base station (BS) is equipped with fully digital beamforming arrays and the number of Tx antenna elements N_{Tx} for DL transmission is much larger than that of Rx elements N_{Rx} for UL reception. As shown in Figure 3, power ratio R extracted from 28 GHz simulation data reduces with increase of array size gap, and in 50% of cases, the R values equal to 0 dB. Thus, angle reciprocity of UL and DL radio channel still hold with a focus on beam directions.

4.2 Impact on Time Dispersion

Time dispersion is an import channel characteristic for optimal adaption of the transmission waveform. For example,

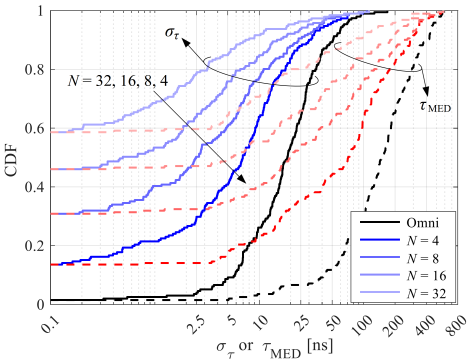

Figure 4. Empirical CDFs of max beam DS and MED for 142 GHz measured radio channels weighted by beam patterns of N-element ULA.

large root mean squared (RMS) delay spread (DS) σ_τ or maximum excess delay (MED) τ_{MED} causes inter-symbol interference, which can be mitigated via inserting cyclic prefix before data symbols, resulting in the reduction of the spectrum efficiency.

Based on estimated beam direction information, we first steer a beam pattern to a desired beam direction, e.g., the direction having maximum received power $\varphi_{\mathrm{rx,max}}$ as depicted in Figure 2. Then, propagation path gains will be weighted with steered beam pattern, resulting in the beam-weighted channel as

$$\tilde{P}(\tau, \phi_{\mathrm{rx}} | \varphi_{\mathrm{rx,max}}) = \sum_{l=1}^{L} p_l G(\phi_{\mathrm{rx},l} - \varphi_{\mathrm{rx,max}}) \delta(\tau - \tau_l) \cdot \delta(\phi_{\mathrm{rx}} - \phi_{\mathrm{rx},l}) \quad (5)$$

In Figure 2, the red filled circles represent the PAS weighted by the beam pattern of 4-element ULA steered towards the maximum beam direction, i.e., $\varphi_{\mathrm{rx,max}} = 147°$. Figure 4 shows the empirical CDFs of beam-weighted DS and MED using 142 GHz measured channel data. It is shown that beamforming significantly reduces time dispersion compared with the results for omnidirectional channels. Meanwhile, the analysis indicated a clear inverse proportionality between the number of elements N in ULA and time dispersion parameters.

5 Conclusion

In this paper, we summarize our recent works on the analysis of beamforming impact on mmWave and sub-THz wireless transmission scheme design and draw design insights from a radio channel point of view. We estimate the number of beam directions that measured and simulated mmWave/sub-THz radio channels can support to establish reliable communication links. Based on the proposed beam direction-based similarity metric, it is feasible to leverage LF spatial channel information for HF beam search only if it does not exist pronounced HPBW difference between HF and LF beams. Besides, angle reciprocity of UL and DL radio channel still holds when using asymmetric transceiver based on the analysis of UL and DL radio channel similarity with the same metric. The significant reduction of DS and MED can be observed from beam-weighted channels in comparison with omnidirectional propagation channels.

Acknowledgements

This work was partly supported by the Research Council of Finland (former Academy of Finland) Multipath project (Grant no. 348980) and 6G Flagship Programme (Grant no. 346208). This work has been partly performed under the framework of EU COST INTERACT CA20120 action.

References

[1] M. Giordani, M. Polese, A. Roy, D. Castor, and M. Zorzi, "A tutorial on beam management for 3GPP NR at mmWave frequencies," *IEEE Commun. Surveys Tuts.*, vol. 21, no. 1, pp. 173–196, 1 st Quart. 2019.

[2] M. Shafi *et al.*, "Microwave vs. millimeter-wave propagation channels: Key differences and impact on 5G cellular systems," *IEEE Commun. Mag.*, vol. 56, no. 12, pp. 14–20, Dec. 2018.

[3] "Study on channel model for frequency from 0.5 to 100 GHz," 3GPP, TR38.901 (V17.0.0), Mar. 2022.

[4] M. F. De Guzman, K. Haneda, and P. Kyösti, "Measurement-based mimo channel model at 140 GHz (V1)," Zenodo, Feb. 2023. [Online]. Available: https://doi.org/10.5281/zenodo.7640353

[5] P. Kyösti, M. F. De Guzman, K. Haneda, N. Tervo, and A. Pärssinen, "How many beams does sub-THz channel support?" *IEEE Antennas Wireless Propag. Lett.*, vol. 21, no. 1, pp. 74–78, Jan. 2022.

[6] P. Zhang *et al.*, "Out-of-band information aided mmWave/THz beam search: A spatial channel similarity perspective," *IEEE Commun. Mag.*, pp. 1–7, 2023.

[7] P. Kyösti, P. Zhang, A. Pärssinen, K. Haneda, P. Koivumäki, and W. Fan, "On the feasibility of out-of-band spatial channel information for millimeter-wave beam search," *IEEE Trans. Antennas Propag.*, vol. 71, no. 5, pp. 4433–4443, May 2023.

[8] W. Hong *et al.*, "The role of millimeter-wave technologies in 5G/6G wireless communications," *IEEE J. Microw.*, vol. 1, no. 1, pp. 101–122, Jan. 2021.

[9] P. Zhang *et al.*, "A modular COTS-based high-efficient sub-THz channel sounder and experimental validations," in *Proc. 17th Eur. Conf. Antennas Propag. (EuCAP)*, Mar. 2024, pp. 1–5.

[10] N. González-Prelcic, A. Ali, V. Va, and R. W. Heath, "Millimeter-wave communication with out-of-band information," *IEEE Commun. Mag.*, vol. 55, no. 12, pp. 140–146, Dec. 2017.